ARTICLE

A. A. Toye · J. D. Lippiat · P. Proks · K. Shimomura ·
L.Bentley · A. Hugill · V. Mijat · M. Goldsworthy ·
L.Moir · A. Haynes · J. Quarterman · H. C. Freeman ·
F. M. Ashcroft · R. D. Cox

A genetic and physiological study of impaired glucose homeostasis control in C57BL/6J mice

Abstract *Aims/hypothesis:* C57BL/6J mice exhibit impaired glucose tolerance. The aims of this study were to map the genetic loci underlying this phenotype, to further characterise the physiological defects and to identify candidate genes. *Methods:* Glucose tolerance was measured in an intraperitoneal glucose tolerance test and genetic determinants mapped in an F2 intercross. Insulin sensitivity was measured by injecting insulin and following glucose disposal from the plasma. To measure beta cell function, insulin secretion and electrophysiological studies were carried out on isolated islets. Candidate genes were investigated by sequencing and quantitative RNA analysis. *Results:* C57BL/6J mice showed normal insulin sensitivity and impaired insulin secretion. In beta cells, glucose did not stimulate a rise in intracellular calcium and its ability to close K_{ATP} channels was impaired. We identified three genetic loci responsible for the impaired glucose tolerance. Nicotinamide nucleotide transhydrogenase (*Nnt*) lies within one locus and is a nuclear-encoded mitochondrial proton pump. Expression of *Nnt* is more than sevenfold and fivefold lower respectively in C57BL/6J liver and islets. There is a missense mutation in exon 1 and a multi-exon deletion in the C57BL/6J gene. Glucokinase lies within the *Gluchos2* locus and shows reduced enzyme activity in liver. *Conclusions/interpretation:* The C57BL/6J mouse strain exhibits plasma glucose intolerance reminiscent of human type 2 diabetes. Our data suggest a defect in beta cell glucose metabolism that results in reduced electrical activity and insulin secretion. We have identified three loci that are responsible for the inherited impaired plasma glucose tolerance and identified a novel candidate gene for contribution to glucose intolerance through reduced beta cell activity.

Keywords C3H/HeH · C57BL/6J · *Gck* · *Gluchos* · Insulin · Islet · K_{ATP} channel · *Nnt* · Type 2 diabetes

Abbreviations Gapdh: Glyceraldehyde-3-phosphate dehydrogenase · Gck: Glucokinase · IPGTT: Intraperitoneal glucose tolerance test · K_{ATP}: ATP-sensitive K^+ · Nnt: Nicotinamide nucleotide transhydrogenase · QTL: Quantitative trait locus · TCA: Tricarboxylic acid (Krebs) cycle

A. A. Toye · L. Bentley · A. Hugill · V. Mijat · M. Goldsworthy ·
L. Moir · A. Haynes · J. Quarterman · H. C. Freeman ·
R. D. Cox
Medical Research Council,
Harwell, Didcot, Oxfordshire, UK

J. D. Lippiat · P. Proks · K. Shimomura · F. M. Ashcroft
University Laboratory of Physiology,
Parks Road, Oxford, UK

R. D. Cox (✉)
MRC Mammalian Genetics Unit,
Medical Research Council,
Harwell, Didcot, Oxfordshire, OX11 0RD, UK
e-mail: r.cox@har.mrc.ac.uk
Tel.: +44-1235-841184
Fax: +44-1235-841200

Introduction

Insulin release from pancreatic beta cells is stimulated by increased beta cell uptake and metabolism of glucose. The consequent changes in the intracellular concentrations of adenine nucleotides cause closure of ATP-sensitive K^+ (K_{ATP}) channels in the beta cell plasma membrane. In turn, this leads to membrane depolarisation, opening of voltage-gated Ca^{2+} channels, Ca^{2+} influx, fusion of insulin secretory vesicles with the plasma membrane and insulin secretion. Normally, insulin secretion in response to elevated plasma glucose is biphasic. Intracellular messengers controlling K_{ATP} channel-dependent first-phase insulin secretion also regulate second-phase insulin secretion. However, additional K_{ATP} channel-independent messengers are also involved [1]. There is evidence that loss of first-phase insulin secretion leads to postprandial hyperglycaemia and is com-

mon in patients with type 2 diabetes and individuals with impaired glucose tolerance [2].

Defects in beta cell function are found in monogenic diabetes, such as maturity-onset diabetes of the young (reviewed in Ref. [3]) and permanent neonatal diabetes. It is also apparent that abnormalities in insulin secretion and beta cell function contribute to the onset and development of polygenic type 2 diabetes [3]. In type 2 diabetes there is gradual progression from normal glucose tolerance to impaired glucose tolerance and subsequently overt diabetes. This is associated with a progressive decline in beta cell function and reduced insulin secretion. Insulin resistance may enhance the risk of diabetes by placing an increased demand upon the beta cell, but by itself does not result in diabetes. The genetic defects that produce inappropriate homeostatic control in type 2 diabetes are poorly understood (reviewed in Refs. [3, 4]).

Animal models of glucose intolerance provide valuable information about glucose homeostasis that can ultimately be applied to human diabetes. The C57BL/6J mouse exhibits defects in glucose tolerance that are independent of obesity [5, 6]. Feeding C57BL/6J mice with high-fat diets results in insulin resistance, increased fasting plasma glucose levels and diabetes [7–10]. On a high-fat diet these mice also show higher weight gain per energy intake [11], higher weight gain when the same amount of energy is given as fat [12], and higher fat and lower protein and water body composition [13] than A/J mice. Insulin action was also reduced by between 32% and 60% in C57BL/6J mice after 9 months on a high-fat diet [9]. Interestingly, however, C57BL/6J mice are actually more insulin-sensitive than AKR/J mice [14] and DBA/2 or 129X1 mice [15].

On normal diets, C57BL/6J mice appear to have normal free-fed plasma insulin levels, but postprandial first-phase insulin release is impaired when compared to glucose-tolerant control strains, including C3H [5, 16]. Second-phase insulin release is also impaired in comparison with AKR/J [14] and DBA/2 [6] mice, but is not significantly different to C3H mice (at least at 8 weeks of age) [5]. A defect in first-phase insulin secretion also appears to be present in C57BL/6J mice fed a high-fat diet [17], and is accompanied by an unchanged insulin response and delayed glucose clearance over the first 4 weeks of a high-fat diet [18]. Recent physiological [9] and genetic studies [8, 19] also suggest that insulin and plasma glucose levels are poorly correlated. Classification of C57BL/6J mice on a high-fat diet into (1) lean non-diabetic (12%), (2) lean diabetic (12%), (3) obese diabetic (about 50%), and (4) intermediates has allowed a microarray transcript profiling comparison to be made and shown striking differences in gene expression between the groups [20]. These data suggest a differential metabolic adaptation, not wholly under genetic control, that contributes to the observed phenotypic diversity in this strain [20].

In summary, C57BL/6J mice represent an important model of diet-induced diabetes, which also exhibits defects in glucose tolerance on a normal diet. This model develops insulin resistance on a high-fat diet and appears to have a complex insulin secretion deficit on normal and high-fat diets.

Here, we use genetic mapping of F2 intercross mice, physiological studies of whole mice, studies of isolated liver and pancreatic tissues, and candidate gene analyses, to define more precisely the genetic basis of glucose intolerance in C57BL/6J mice.

Materials and methods

Animals Mice were kept in accordance with UK Home Office welfare guidelines and project license restrictions. C57BL/6J mice were obtained from Jackson Laboratory (Bar Harbor, ME, USA) in 1999. C3H/HeH mice were from the Harwell (Oxfordshire, UK) stock. Mice were maintained under controlled conditions and had free access to a commercial diet (maintenance chow; Special Diet Services, Essex, UK) containing 2.6% saturated fat.

Genotyping Genomic DNA was extracted from mouse tail tissue using a Qiagen DNeasy tissue kit (Qiagen, Hilden, Germany). Mice were genotyped by SSLP analysis. Primer sequences were obtained from published records [21]. PCR products were analysed using an ABI 377 sequencer and Genescan and Genotyper software and protocols (Applied Biosystems Europe, Warrington, Cheshire, UK). Markers were spaced at a median interval of 11 cM, with an average interval of 14.6 cM and a largest interval of 46.7 cM.

Linkage analysis Phenotype and genotype data were maintained in Microsoft Excel, SPSS and MapManager QTX ([22]; see http://www.mapmgr.roswellpark.org/) formats. Genetic maps were constructed using the published map order of markers (http://www.informatics.jax.org). Linkage between markers and phenotypes was evaluated using a single marker, and interval mapping features of MapManager. Thresholds for defining linkage were as outlined by Lander and Kruglyak [23], with additional permutation tests [22] where stated. Empirical thresholds were based on analysis of 1,000 permutations of the original data set. Thresholds derived from free model permutation were LRS 15.7 (LOD 3.4) for T0 glucose, LRS 16.1 (LOD 3.5) for T30 glucose, LRS 15.5 (LOD 3.4) for T60 glucose, LRS 15.7 (LOD 3.4) for AUC glucose and LRS 16.9 (LOD 3.7) for T30 insulin.

Intraperitoneal glucose tolerance tests Mice were fasted overnight, weighed, and a blood sample collected by tail venipuncture under local anaesthetic (lignocaine; Biorex, Middlesex, UK) using lithium-heparin microvette tubes (Sarstedt, Numbrecht, Germany) to establish a baseline glucose level 'T0'. The mice were then injected intraperitoneally with 2 g glucose/kg body weight and blood samples taken at 15, 30, 60 and 120 min after the injection to monitor the rate of glucose clearance. Plasma glucose and insulin were measured using a Beckman Glucose analyser and a Mercodia Ultra-Sensitive Mouse ELISA kit.

Insulin tolerance test Insulin tolerance tests on free-fed mice were performed as described [6].

Islet cell isolation Mice were killed by cervical dislocation. The pancreas was removed and islets or dissociated islet cells were prepared and cultured as previously described [24]. Cells were exposed to glucose-free solution for 15 min prior to experiment.

Insulin secretion studies Insulin secretion from isolated islets (ten islets/well) was measured during 1-h static incubations in Krebs–Ringer Buffer (in mmol/l: 118.5 NaCl, 2.54 $CaCl_2$, 1.19 KH_2PO_4, 4.74 KCl, 25 $NaHCO_3$, 1.19 $MgSO_4$, 10 HEPES, pH 7.4) containing either 2 or 10 mmol/l glucose. Each glucose concentration was replicated five to eight times. Samples of the supernatant were assayed for insulin. Insulin content was extracted using 95 : 5 ethanol/acetic acid. Insulin was measured using a Mouse Insulin ELISA kit (Mercodia, Uppsala, Sweden).

Fura-2 imaging Islet cells were cultured on 35-mm Fluorodishes (World Precision Instruments, Stevenage, UK) and incubated with 3 µmol/l Fura-2-AM (Molecular Probes, Paisley, UK) for 40 min at 37°C. They were imaged at room temperature (20–24°C) using a fluorescence system (Ion-Optix, Boston, MA, USA), with 340 and 380 nm dual excitation. The 510-nm emission ratio was collected at 1 Hz. Background subtraction was performed by measuring fluorescence from a cell-free region in the field of view. Cells were perfused continuously with extracellular solution (as in perforated-patch experiments), plus glucose or tolbutamide as indicated. Only data from cells that responded to 500 µmol/l tolbutamide were analysed.

Electrophysiology Glucose concentration–response relations for whole-cell K_{ATP} currents were measured using the perforated patch configuration of the patch-clamp technique [25]. The pipette solution contained (mmol/l): 70 K_2SO_4, 1 $CaCl_2$, 1 $MgCl_2$, 10 NaCl, 10 HEPES (pH 7.2 with KOH), and amphotericin B (0.24 mg/ml). The extracellular (bath) solution contained (mmol/l): 137 NaCl, 5.6 KCl, 2.6 $CaCl_2$, 1.2 $MgCl_2$, 10 HEPES (pH 7.4 with NaOH) plus glucose as indicated. Currents were filtered at 3 kHz and digitised at 1 kHz. The K_{ATP} component of the whole-cell current was taken as the current blocked by 200 µmol/l tolbutamide.

The ATP sensitivity of K_{ATP} channels was measured at −60 mV in inside–out patches. Currents were digitised at 5 kHz and filtered at 2 kHz. The pipette (extracellular) contained (mmol/l): 140 KCl, 2.6 $CaCl_2$, 1.2 $MgCl_2$, 10 HEPES (pH 7.4 with KOH). The bath (intracellular) solution contained (mmol/l): 107 KCl, 1 $MgCl_2$, 1 $CaCl_2$, 10 HEPES (pH 7.2 with KOH), and K_2ATP as indicated.

Concentration–response relations were obtained by alternating test solutions with control (glucose- or ATP-free) solution. The control conductance was taken as the mean of that obtained in control solution before and after application of the test agent. The current in the presence of glucose or nucleotide (I) was plotted as a fraction of that obtained in control solution (I_C). Data were the best fit with the Hill equation

$$I/I_C = 1 \Big/ \left(1 + [\{X\}/\mathrm{IC}_{50}]^h \right)$$

where $\{X\}$ is the concentration of glucose or ATP, IC_{50} is the concentration giving half-maximal inhibition of the current and h is the Hill coefficient. Data are given as means±1SEM.

Quantitative RT-PCR Quantitative RT-PCR was performed using ABI SYBR Green on an ABI PRISM 7700 Sequence Detection System (Applied Biosystems). To quantitate nicotinamide nucleotide transhydrogenase (*Nnt*), it was PCR-amplified from cDNA (RT-PCR), together with an endogenous control *Gapdh* (glyceraldehyde-3-phosphate dehydrogenase). RT-PCR primers listed in 5′ to 3′ orientation are for *Gapd*; *Gapd*888F-CCTGCGACTTCAACAG CAACT and *Gapd*979RV-CCAGGAAATGAGCTTGAC AAA; and for *Nnt*: *Nnt*Xn5intF-GATAGTTGGTGGTGG CGTTG and *Nnt*Xn6intR-GATGTCCACCTCCTTGCACT.

The *t*-tests for significant differences between strains are based on RQ (*Nnt*/*Gapd*) values. Relative RQ is the ratio of the C3H/HeH RQ relative to that for C57BL/6J.

Statistical analysis and multilocus model Multiple regression was performed by univariate ANOVA using the GLM feature of SPSS. *F* statistics were based on type III sums of squares. All markers that exceeded LOD 1.9 suggestive linkage threshold [23] were included in the regression model. Terms not significant at the 0.1% level were sequentially eliminated to produce the final multiple regression model. C57BL/6J homozygotes were coded 0.5, C3H/HeH homozygotes were coded −0.5 and heterozygotes were coded 0 in all regression analyses.

Results

Whole-animal studies

To identify suitable strains for mapping loci that determine obesity-independent impaired glucose tolerance, we surveyed four nonobese inbred mouse strains (C57BL/6J, C3H/HeH, DBA/2 and BALB/c) for variation in glucose tolerance during an intraperitoneal glucose tolerance test (IPGTT). Male mice were less glucose-tolerant than female (data not shown). Consistent with previous studies [5, 16], male C57BL/6J mice were also significantly less glucose-tolerant than other strains (Fig. 1a; $p<0.05$). Therefore, we used genetic analysis to identify loci that determine glucose homeostasis in 260 F2 male mice produced by intercrossing first the C57BL/6J strain with a control strain (C3H/HeH), and then their F1 progeny.

To elucidate whether epigenetic effects determine C57BL/6J glucose intolerance, we first compared the F1 offspring of C57BL/6J mothers with those of C3H/HeH mothers (Fig. 1b). We saw no significant differences between

a

b
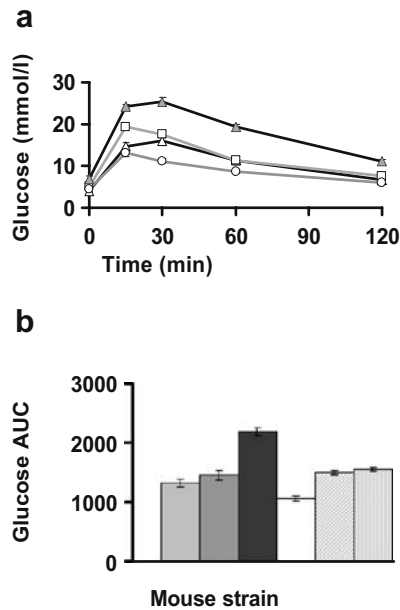
Fig. 1 Male mice at age 12 weeks showing (**a**) results of intra-peritoneal glucose tolerance tests (IPGTT) and (**b**) the IPGTT AUC in $min·mol^{-1}·l^{-1}$ (mean value profiles of four inbred strains). (**a**) *Open circles*, DBA/2 (*n*=10); *open triangles*, BALB/C (*n*=10); *open squares*, C3H/HeH (*n*=10); *filled triangles*, C57BL/6J (*n*=10). *Bars* (**b**) represent from left to right: BALB/C (*n*=10); C3H/HeH (*n*=10); C57BL/6J (*n*=10); DBA/2 (*n*=10); F1 (B/C, *n*=53) male offspring of a cross between C57BL/6 mothers and C3H/HeH fathers; F1 (C/B, *n*=72) F1 male offspring of a cross between C3H/HeH mothers and C57BL/6 fathers. *Y-error bars* represent SEM

male (*n*=125) and female mice (*n*=91, *p*<0.05). F1 males (*n*=125) had significantly (*p*<0.0001) lower plasma glucose than their C57BL/6J mothers (B, *n*=10), but not their C3H/

HeH parents (C, *n*=10) (Fig. 1b). We then examined the F2 phenotypes in the four possible F1 cross-combinations (CB×CB, CB×BC, BC×CB and BC×BC) in order to evaluate epigenetic effects in this generation. The T30, T60, T120 min and AUC glucose phenotypes were significantly (albeit weakly, i.e., close to the <0.05 threshold) different in some, but not all, of the pairwise comparisons. For T0, two of the six phenotype comparisons were significantly different (*p*<0.01) and one at a *p* value of less than 0.05 (data not shown). Thus there may be some weak epigenetic effects that influence the T0 phenotype in particular. All four cross-combinations are equally represented in the F2 population for linkage analysis.

To identify contributing loci, 260 F2 male mice were genotyped with 84 markers [21], providing genome coverage at an average intermarker distance of 15 cM. Plasma glucose levels during an IPGTT were significantly higher at T30 and T60 in the C57BL/6J strain, and were linked to D13Mit77 (LRS 22.8) (Table 1, Fig. 2). This locus was named *Gluchos1* for glucose homeostasis locus-1.

The fasting plasma glucose level was linked to chromosome 11 (D11Mit 2, LRS 23.7) and is designated *Gluchos2* (Table 1, Fig. 2). Plasma glucose levels at T15 and T120 were not significantly linked to any locus.

The plasma insulin level at T30 provides a measure of second-phase insulin secretion [5, 16]. It was significantly (*p*<0.05, r^2=0.0433, *r*=0.208), but poorly, correlated to plasma glucose at the same IPGTT time point, and linked to a locus on chromosome 9 (D9Mit1001, LRS 30.9), which was named *Gluchos3* (Table 1, Fig. 2). Insulin was correlated with body weight (r^2=0.2319, *r*=0.48) but body weight was not correlated with T30 glucose (r^2=0.0196, *r*=0.014).

Table 1 Genome scan for plasma glucose and insulin QTLs in male mice aged 12 weeks

Plasma trait[a]	Chromosome (locus)	LRS (LOD)[b]	Percentage	*p* value	CI[c]	Add[d]	Dom[e]	Phenotype at closest marker[f]		
								C3H (*n*)	F1 (*n*)	C57BL/6J (*n*)
T0 glucose (mmol/l)	11 (D11Mit2)	23.75 (52)	9	1E−05	23	−0.78	−0.32	4.91±1.87 (66)	5.4±1.89 (139)	6.44±1.81(68)
T30 glucose (mmol/l)	13 (D13Mit77)	22.8 (5)	8	1E−05	24	−2.16	−0.11	17.05±5.14 (71)	18.96±5.16 (126)	21.39±5.2(64)
T60 glucose (mmol/l)	13 (D13Mit262)	22.1 (4.8)	8	2E−05	25	−1.9	−0.5	13.6±4.75 (72)	14.97±4.71 (132)	17.36±4.71 (66)
AUC (min·mmol^{-1} l^{-1})	13 (D13Mit77)	21.3 (4.6)	8	2E−05	26	−180	−19	1,535.76±444 (70)	1,685.45±444 (125)	1,898.31±444 (64)
T30 insulin (ng/ml)	9 (D9Mit1001)	30.9 (6.7)	24	2E−07	20	0.19	−0.15	0.59±0.24(23)	0.3±0.23(61)	0.26±0.27(29)

Free model LOD score profile across autosomes for T0, T30, T60, AUC glucose and T30 insulin measurements. *n*=280 random mice for all glucose traits. *n*=120 mice, 60 each from opposite extremes of AUC distribution, for T30 insulin. Only significant (Lander and Kruglyak [23]) linkages are shown
Percentage % of variance explained by this locus (at D*n*Mit*n* microsatellite marker name)
[a]Measure of blood plasma trait at time indicated or AUC
[b]Likelihood ratio statistic (LOD score)
[c]The interval around the marker, in which the QTL will localise in 95% of attempts to map it
[d]Additive regression coefficient
[e]Dominance regression coefficient
[f]Average±SD phenotype values for the indicated locus marker in the three possible genotype states: C3H homozygous, F1 heterozygous, C57BL/6J homozygous (*n* number of animals)
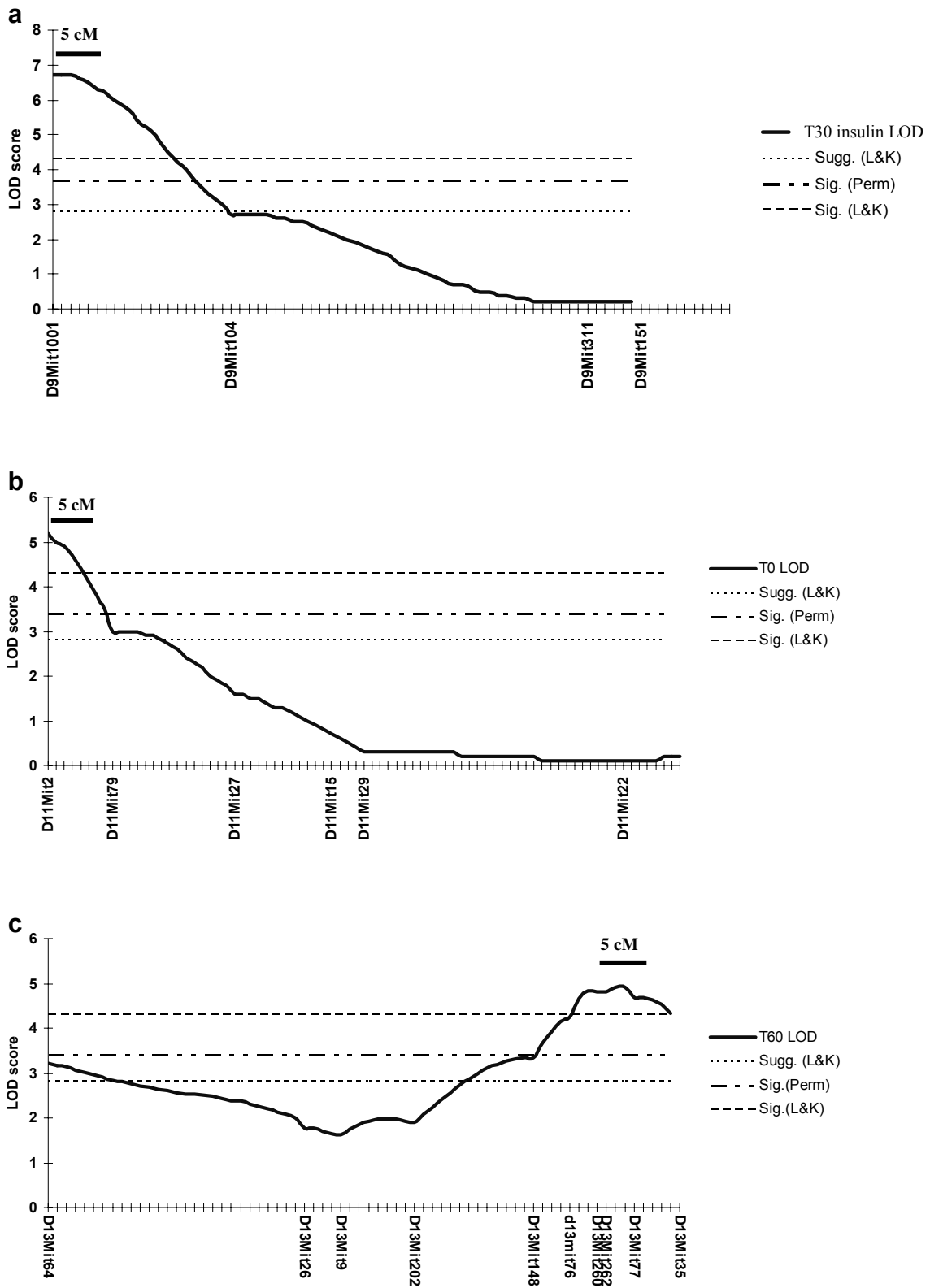
Fig. 2 Interval maps of T30 (**a**), T0 (**b**) and T60 (**c**) glucose on chromosomes 9, 11 and 13, respectively. *Sugg.* (L&K) and *Sig.* (L&K) are widely accepted thresholds for declaring suggestive and significant linkage (Lander and Kruglyak [23]). *Sig.* (perm) is the empirical false discovery threshold for declaring significant T60 glucose linkage in the current dataset and was derived from analysis of 1,000 permutations of the original dataset

Glucose intolerance can arise through the coordinated action of several loci [19, 26]. We therefore explored the role of gene interactions. The combined action of *Gluchos1* and seven additional loci (suggestive of linkage to plasma glucose) explains 35% of the variation in AUC, which is a measure of postprandial plasma glucose clearance (Table 2).

We explored whether insulin sensitivity was affected in C57BL/6J mice using an intraperitoneal insulin tolerance test. C57BL/6J mice (n=10) had significantly higher free-fed plasma glucose prior to insulin injection than C3H/HeH mice ($p<0.001$; Fig. 3), and responded significantly better to insulin within the first 10 min ($p<0.03$). We saw no significant difference ($p>0.05$) between strains in plasma glucose levels in response to insulin at 10, 20, 30 and 60 min after insulin injection.

We therefore looked for differences in insulin secretion by carrying out an IPGTT, taking samples for insulin analysis at 0, 10, 20 and 30 min after glucose injection (Table 3). Insulin secretion by C57BL/6J mice was significantly lower (for the same glucose challenge per gram bodyweight) than for C3H/HeH mice. On average C57BL/6J mice were about 6 g lighter than C3H/HeH mice. Thus our data favour a defect in insulin secretion rather than insulin action.

Isolated islet studies

To test the idea that a defect in beta cell function underlies the glucose intolerance of C57BL/6J mice, we compared the ability of glucose to stimulate insulin secretion from islets
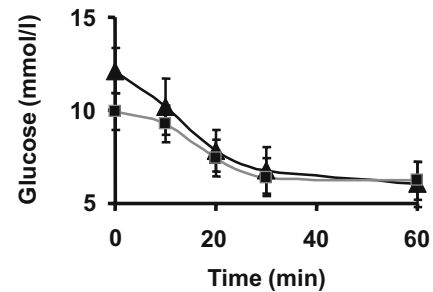
Fig. 3 Plasma glucose dynamics of 12-week-old free-fed male mice in an insulin tolerance test. Free-fed plasma glucose is significantly higher in C57BL/6J mice (*filled triangles*, p=0.001). Plasma glucose clearance is significantly more rapid in C57BL/6 mice than C3H/HeH mice (*filled squares*) in the first 10 min of the test (p=0.03). There was no significant difference in plasma glucose clearance rate or level at any other time points. *Y-error bars* represent SD values

isolated from C3H/HeH and C57BL/6J mice. Figure 4 shows that there was no difference in basal secretion (at 2 mmol/l glucose) between the two mouse strains, but that insulin secretion in response to 10 mmol/l glucose was impaired in C57BL/6J islets in comparison with C3H/HeH islets ($p<0.01$). The data are representative of three experiments.

We next measured the effect of glucose on intracellular calcium, using the calcium indicator Fura 2. Figure 5a shows representative recordings of the fluorescence ratio (F_{340}/F_{380}) from islet cells of both mouse strains. Although both responded to 500 μmol/l tolbutamide with a rise in $[Ca^{2+}]_i$, only beta cells from C3H/HeH mice showed an increase in $[Ca^{2+}]_i$ following exposure to 5 or 10 mmol/l

Table 2 ANOVA table for regression of multiple QTL on plasma glucose tolerance AUC (min·mol^{-1}·l^{-1})

Factor	Type III SS	Degrees of freedom	Mean square	F statistic[a]	p value[b]	Exp (%)[c]
Corrected model	22,412,056.41	24	933,835.68	6.642044	7.56141E−16	41.36
Intercept	427,405,402.26	1	427,405,402.26	30.39.984	4.6828E−133	
D13Mit77	3,394,911.79	2	1,697,455.90	12.07341	1.04285E−05	9.65
D13Mit64	492,705.72	2	246,352.86	1.752221	0.175735623	1.53
D19Mit41	1,032,581.65	2	516,290.82	3.672195	0.026949558	3.15
D13Mit64 * D19Mit41	4,354,787.68	4	1,088,696.92	7.743517	7.2731E−06	12.05
D2Mit200	101,147.70	2	50,573.85	0.359714	0.698274735	0.32
D9Mit311	578,235.94	2	289,117.97	2.056394	0.130301167	1.79
D2Mit200 * D9Mit311	2,895,102.84	4	723,775.71	5.147961	0.000548529	8.35
D7Mit91	2,844,846.90	2	1,422,423.45	10.1172	6.19226E−05	8.22
D6Mit268	3,263,969.15	2	1,631,984.57	11.60773	1.58957E−05	9.32
D16Mit146	1,839,186.94	2	919,593.47	6.540744	0.001732053	5.47
Error	31,774,385.23	226	140,594.62			
Total	781,242,405.41	251				
Corrected total	54,186,441.64	250				

r^2=0.414
(Adjusted r^2=0.351)

Factor is source of plasma glucose AUC variation; SS is type III sum of squares adjusting for all other terms in the model
[a]Based on adjusted sum of squares
[b]Based on the F distribution
[c]Estimate of variance explained by a factor or 'eta square', expressed in percentage terms (Exp%=100×SSfactor/[SSfactor+SSerror])

**Table 3** Male C57BL/6J mice secrete less insulin than C3H/HeH mice in response to a glucose challenge in an IPGTT

Strain	Body weight, g±SD***	Plasma insulin at timepoints in an IPGTT±SD (in ng/ml)			
		0 min**	10 min**	20 min**	30 min*
C3H/HeH (n=8)	31.77±0.99	0.46±0.22	0.81±0.50	1.00±0.57	0.63±0.44
C57BL/6J (n=8)	25.45±1.18	0.19±0.00	0.19±0.00	0.32±0.32	0.23±0.06

Mice were approximately 11.5 to 13 weeks old. The lower sensitivity of the insulin ELISA assays is 0.19 ng/ml and thus the levels of insulin in C57BL/6J mice at 0 and 10 min may actually be lower than shown. Differences are significant at the values of *≤0.05, **≤0.01 and ***≤0.001

glucose. This explains the lack of insulin secretion in response to 10 mmol/l glucose of C57BL/6J islets. The mean increase in $[Ca^{2+}]_i$ produced by tolbutamide was not significantly different (t-test) between the two strains (Fig. 5b). In contrast, responses to 5 and 10 mmol/l glucose were significantly different ($p<0.05$). Furthermore, oscillations in $[Ca^{2+}]_i$ on exposure to 10 mmol/l glucose were observed in seven of 11 C3H/HeH beta cells, but were absent from all seven C57BL/6J cells studied. These data indicate that the loss of insulin secretion derives from the failure of glucose to stimulate a rise in intracellular calcium. Furthermore, because tolbutamide elicits an equivalent rise in $[Ca^{2+}]_i$ in both mouse strains, the data further suggest that glucose fails to close K_{ATP} channels and thereby elicit membrane depolarisation and Ca^{2+} entry.

To examine this possibility, we studied the ability of glucose to close K_{ATP} channels in C3H/HeH and C57BL/6J beta cells, using the perforated patch configuration to maintain metabolism intact. Strikingly, K_{ATP} currents in C57BL/6J beta cells were significantly less sensitive to glucose than those of C3H/HeH beta cells, the IC_{50} being 24.7±2.9 mmol/l (n=13) and 5.7±0.2 mmol/l (n=6), respectively (Fig. 6a, b). This result is consistent with the higher fasting glucose levels and lower glucose tolerance of C57/BL6 mice. To explore if this difference in glucose

sensitivity is due to differences in beta cell metabolism or in the K_{ATP} channel itself, we measured the concentration–response curve for channel inhibition by ATP. Figure 6c, d shows that half-maximal inhibition of C57BL/6J K_{ATP}
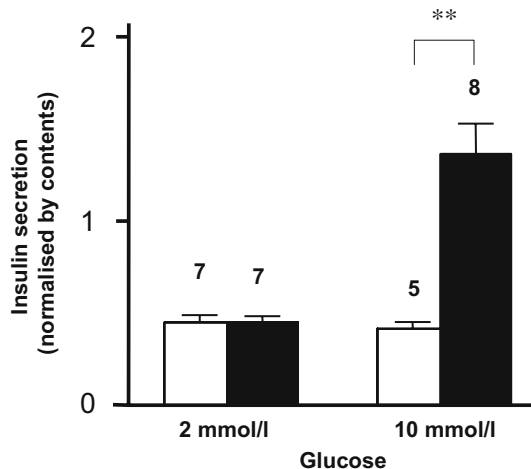
Fig. 4 Insulin secretion in response to glucose is impaired in isolated islets from C57BL/6J compared to C3H/HeH mice. *White bars*, C57BL/6J islets; *black bars*, C3H/HeH islets. The *numbers* above the bars indicate the numbers of replicated wells (each well contained ten islets). *Y-error bars* represent SEM. **$p<0.01$
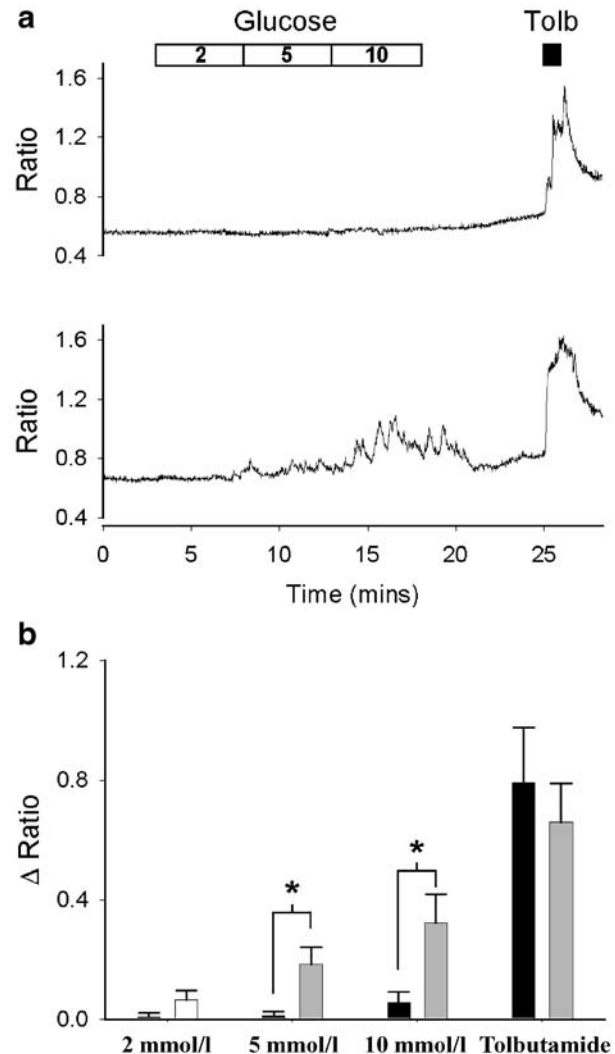
Fig. 5 a Representative changes in intracellular Ca^{2+}, measured by Fura-2 fluorescence, in response to glucose and tolbutamide in single beta cells isolated from C57BL/6J (*upper panel*) and C3H/HeH (*lower panel*) mice. The *bar* indicates when glucose (2, 5, 10 mmol/l) and tolbutamide (500 μmol/l) were applied. Mean change (**b**) in fluorescence ratio in response to glucose (2, 5 and 10 mmol/l) or tolbutamide (as indicated) in beta cells from C57BL/6J mice (*black bars*, n=7) and C3H/HeH mice (*grey bars*, n=11). *$p<0.05$ (t-test)

a

b

c

d
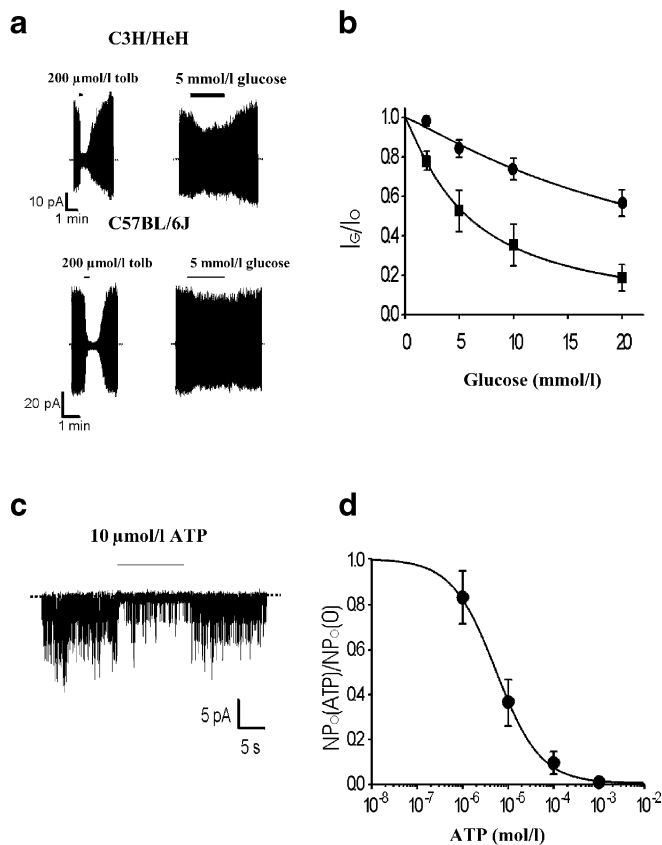
Fig. 6 Effects of glucose and ATP on K_{ATP} currents. **a** Representative whole-cell perforated patch recordings from a C3H/HeH and a C57BL/6J mouse beta cell in response to ±20 mV pulses from −70 mV. Glucose (5 mmol/l) or tolbutamide (200 μmol/l) were applied to the external solution as indicated. The *dotted lines* show the zero-current level. **b** Mean glucose concentration–response relationships for whole-cell K_{ATP} currents from C57BL/6J (*circles*, n=13) or C3H/HeH (*squares*, n=6) beta cells. Current (I) is expressed as a fraction of the mean (I_0) of that obtained in control solution before and after exposure to glucose. The lines are the best fit of the Hill equation to the data. For C57BL/6J mice, IC_{50}=24.7±2.9 mmol/l, h=1.15±0.16 (n=13). For C3H/HeH mice, IC_{50}=5.7±0.2 mmol/l, h=1.16±0.04 (n=6). Single-channel currents (**c**) recorded at −60 mV from inside–out patches excised from a C57BL/6J or CH3/HeH beta cell. ATP (10 μmol/l) was applied to the intracellular solution as indicated. The *dotted line* indicates the zero-current level. Mean ATP concentration–response relationship (**d**) for K_{ATP} channels from C57BL/6J beta cells. Channel activity ($NPo[ATP]$) is expressed as a fraction of the mean (NPo) of that obtained in control solution before and after exposure to ATP. The *line* is the best fit of the Hill equation to the data: IC_{50}=5.7±0.5 μmol/l, h=0.89±0.06 (n=5). *Y-error bars* represent SEM

channels by ATP (IC_{50} 10 μmol/l) is similar to that observed for NMRI mice [27] and for cloned K_{ATP} channels [28]. This suggests that the defect in C57BL/6J mice lies prior to K_{ATP} channel closure, probably at the level of beta cell metabolism.

Candidate gene studies

Gluchos1 (chromosome 13) In a 5-cM sweep around *Gluchos*1 on chromosome 13 at 65±12 cM we identified several potential candidate genes: in particular, the transcription factor islet gene enhancer protein 1 (*Isl1*), (113 Mbp) and *Nnt* (64 cM or 116 Mbp). The coding sequence of *Isl1* was sequenced and no mutations found.

We sequenced the coding region of *Nnt* and found two mutations. First, an exchange of T (C3H/HeH) for C (C57BL/6J) at nt 104 of exon 1 that results in a missense methionine to threonine mutation at amino acid 35 of the protein. This mutation is located in the mitochondrial leader peptide sequence of the *Nnt* precursor protein [29]. The second mutation was found in islet and liver cDNA PCR-amplified between exon 5 and 13, numbered according to the *Nnt* gene structure and sequence that have been derived from 129/SvJ mice ([30]; GENBANK AAF72982, AF257137 –AF257157). The amplified fragment was ~508 bp from C57BL/6J but ~1,261 bp from C3H/HeH cDNA. Sequencing of these products confirmed that exons 7 to 11 were completely missing in the C57BL/6J fragment, although the transcript remained in frame between exons 6 and 12 (see electronic supplementary material [ESM], link on first page of this article). In silico analysis of cDNA database sequences from 129/SvJ, NOD, FVB, C57BL/6J and B6CBAF1 mouse strains independently confirmed that most C57BL/6 annotated transcripts also lack a 753-bp segment that encompasses the whole of exons 7 to 11 expected from the structure of the 129/SvJ gene and that of other mouse strains [30]. PCR amplification of exons from genomic DNA of 26 different inbred strains and substrains indicated that only C57BL/6J is missing exons 7 to 11 and that in the other strains all exons are present (data not shown). This is consistent with BLAST searches of the ENSEMBL C57BL/6J mouse sequence (releases v13.30.1, May 2003 and NCBIM 32_feb 2004) that revealed no homology to these exons.

Finally, we assayed the RNA expression level of *Nnt* by RT-PCR, by amplifying a 277-bp fragment bridging exons 5 and 6 of the gene. Gene expression in C3H/HeH compared to C57BL/6J mice was at least sevenfold higher in the liver and approximately fivefold higher in islet RNA (Fig. 7).

Gluchos2 (chromosome 11) Gluchos2 lies in a region of comparative homology with a rat chromosome 14 diabetes quantitative trait locus (QTL), *Dmo3* [31]. There are a number of potential candidate genes that lie under the peak of linkage, most notably *CamK2B* and *Gck*. We sequenced the entire coding sequence of *CamK2B* and found no mutations capable of disrupting protein function. Given the crucial role of glucokinase in glucose homeostasis [32–37], we compared in vitro glucokinase function in liver of 12-week-old male C57BL/6J and C3H/HeH mice. C57BL/6J mice had significantly (p<0.01) lower glucokinase activity despite similar hexokinase activity: glucokinase activity was 16.61±2.144 (SD) mU/mg protein (n=5) for C57BL/6J compared to 22.73±2.09 mU/mg protein (n=4) for C3H/HeH (enzyme activity level was measured using triplicate V_{max} assays). We sequenced the islet promoter and entire coding region of the *Gck* gene in both strains and found one silent polymorphism in C57BL/6J, namely a C-to-G transversion at base 131 of exon 7.

Fig. 7 Quantitative RT-PCR assessment of *Nnt* gene expression in liver (*n*=4 C3H/HeH mice, *n*=4 C57BL/6J mice, fasted *p*<0.01, free-fed *p*<0.01) and isolated islets (approximately 300 islets from each strain pooled to make RNA) of 12-week-old male mice. C3H/HeH, *light grey bars*; C57BL/6, *black bars*. *RQ* is the relative quantitation statistic representing the *Nnt:GAPDH* expression ratio. Relative RQ expresses the ratio of the RQ statistic for the higher expressing strain (C3H/HeH) relative to that for the lower expressing strain (C57BL/6). *Y-error bars* represent SD values
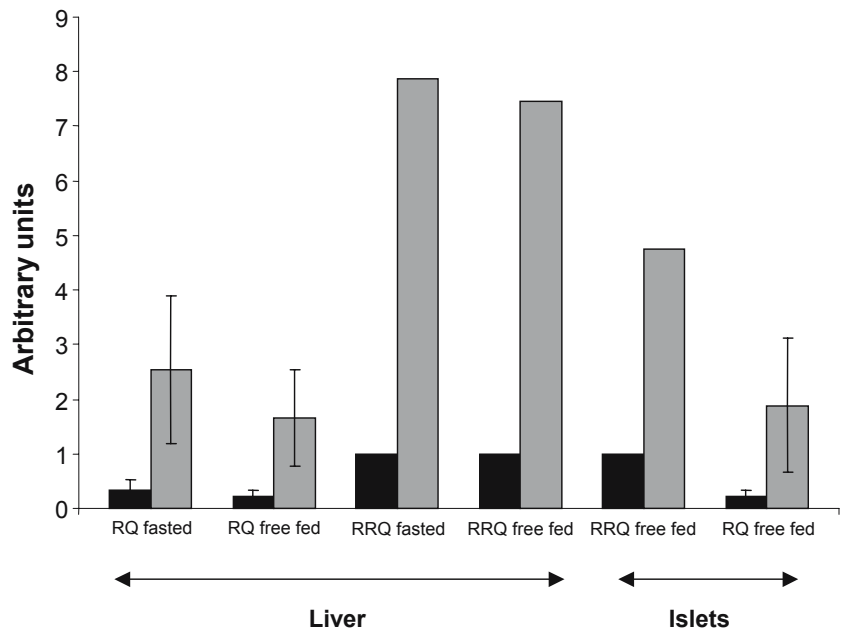
Gluchos3 (chromosome 9) There are a large number of genes in the *Gluchos3* region including several of potential interest. For example, *Atp5l* encodes a subunit of the mitochondrial F0 complex involved in ATP synthesis and proton transport. Given its role in ATP synthesis, and the tight coupling between ATP generation and insulin secretion, it seems a good causal candidate for *Gluchos3*. The *islet-2* gene (a relative of *islet-1*) also lies on chromosome 9, but at the edge of the potential linkage.

Discussion

IPGTT comparisons between four nonobese inbred mouse strains revealed that C57BL/6J mice were less glucose-tolerant than C3H, DBA/2 and BALB/c, and that male mice were significantly less glucose-tolerant than females. Sex differences in glucose tolerance are common and well documented in several mouse strains and are possibly due to hormonal differences [38–40].

Studies on F1 male mice resulting from reciprocal crosses indicated that glucose intolerance in C57BL/6J mice did not appear to be the result of mitochondrial genome, intra-uterine environment or other maternal environment effects on progeny. However, we did observe effects in some of the pairwise comparisons of the four F2 cross-combinations, although the cause of these differences is unknown. Moreover, if the trait data are adjusted to take account of the cross direction effects then reanalysed for linkage, there is no significant change in the mapped QTLs or their LOD scores (data not shown).

In an intercross between nonobese C3H/HeH and C57BL/6J mice we identified three loci that influence glucose homeostasis under fasting conditions (*t*=0, Table 1) and in response to a glucose challenge (*t*=30, *t*=60 and AUC;

Table 1). These were *Gluchos1*, *Gluchos2* and *Gluchos3*, located on chromosomes 13, 11 and 9, respectively.

Other crosses with C57BL/6J or related B6 strains have mapped loci to a number of chromosomes and are summarised in Table 4 [15, 19, 40–44]. These crosses support by replication loci on chromosomes 2, 6, 13 and 19, although strain combination and cross design differences may account for the discordance of the other loci, and within a chromosome could also represent different QTLs. Linkages close to *Gluchos1* on chromosome 13 have been detected in two different studies (Table 4). The locus mapped in the *TallyHo* cross may overlap somewhat in position with ours but actually maps inheritance of *T* alleles contributing to increased nonfasting glucose [40]. In the other cross, the F2 map position overlaps with our locus and corresponds to the inheritance of C57BL/6J alleles causing elevated 30-min glucose and therefore may provide replication [16].

Since the post-glucose-challenge plasma glucose QTL *Gluchos2* and the T30 insulin QTL *Gluchos3* map to different genomic positions they are clearly not directly dependent on one another (indeed, the phenotypes are poorly correlated, *r*=0.28). Given that insulin lowers blood glucose, they might well have been correlated. In our experiments, inheritance of C57BL/6J alleles at *Gluchos3* more than halves plasma insulin and this effect is dominant (Table 1). Further, we have shown that C57BL/6J mice secrete less insulin than C3H/HeH mice over 30 min of a glucose tolerance test (Table 3), consistent with documented defects in glucose-stimulated first- and second-phase insulin secretion, as previously shown for C57BL/6J mice relative to C3H [5, 16], DBA/2 [6] or AKR [14] mice. Insulin tolerance tests showed that administration of exogenous insulin suppresses plasma glucose as effectively in C57BL/6J as in C3H/HeH mice (Fig. 3). This is

Table 4 Summary of significant quantitative trait loci linkages in crosses involving C57BL/6J and related strains

Chr	cM	High allele	Trait and genetic cross	Reference
6	61	C57BL/6J	Increased plasma insulin; F2 C57BL/6J and CAST/Ei. Atherogenic diet	[41]
2	87	C57BL/6J	Increased 30-min IPGTT blood glucose; F2 C57BL/6J and C3H/HeH	[16]
13	45–61	C57BL/6J	As above	[16]
8	72	KK	Increased blood glucose in IPGTT; F2 C57BL/6J and KK-A(y)	[42]
14	10.5	C57BL/6J	Hyperinsulinaemia; F2 C57BL/6J	[43]
			(congenic, doubly heterozygous for IR and IRS-1 knockouts) and 129S6/SvEvTac	
1	38	B6	Increased plasma insulin levels; F2 B6 and 129/Sv carrying heterozygous IR knockout	[44]
2	28	B6	As above	[44]
6	57	B6	As above	[44]
10	48	B6	As above	[44]
12	44	129/Sv	As above	[44]
2	52	BTBR	High fasting plasma insulin; F2 ob/ob population segregating B6 and BTBR alleles	[19]
19	53	BTBR	As above	[19]
16	28	BTBR	High fasting plasma glucose; F2 ob/ob population segregating B6 and BTBR alleles	[19]
13	60	TallyHo (TH)	Increased nonfasted plasma glucose; backcross (C57BL/6J×TH)F1 and TH	[40]
19	50	TallyHo (TH)	Increased nonfasted plasma glucose; backcross (C57BL/6J×TH)F1 and TH or	[40]
			(CASTEi×TH)F1 and TH	

Chr chromosome, *cM* centimorgan, *high allele* the strain contributing the allele associated with an increased phenotype value, *trait and genetic cross* the trait showing linkage and brief details of the genetic mapping cross used

consistent with reports that C57BL/6J mice are more insulin-sensitive than AKR mice on a standard diet [14]. On a high-fat diet, C57BL/6J are still more sensitive to insulin than AKR mice but the difference is reduced. This suggests that the lack of a glucose (T30 and T60) phenotype colocalisation with *Gluchos3* (24% of the T30 insulin variance being controlled by this locus; Table 1) is not due to differences in insulin sensitivity. These data also support the possibility that blood glucose at T30 reflects earlier events in insulin secretion, for example, the rapid first-phase response (or lack of it); that plasma insulin at T30 reflects differences in second-phase insulin secretion; and that the gene being mapped at *Gluchos3* is involved in the latter [1, 45].

The combined action of *Gluchos1* and seven additional loci (suggestive of linkage to plasma glucose) explained 35% of variation in the area under the IPGTT curve. Clearly, postprandial glucose intolerance in C57BL/6J has a complex basis, as multiple unlinked C57BL/6J alleles determine glucose intolerance in the current cross. These results are consistent with other rodent studies [26, 40, 46].

The hypothesis that defective glucose-stimulated insulin release rather than insulin resistance is at least partly responsible for C57BL/6J glucose intolerance on a standard diet is further confirmed by our finding that C57BL/6J islets fail to release insulin in response to 10 mmol/l glucose, unlike C3H/HeH islets ($p<0.01$). We have shown that K_{ATP} channels in C57BL/6J pancreatic beta cells exhibited impaired closure in response to glucose metabolism, which accounts for the smaller increase in intracellular calcium and, in turn, the reduced insulin secretion of these mice. K_{ATP} channels in C57BL/6J beta cells retain normal ATP sensitivity. This suggests that the cause of impaired glucose-stimulated insulin release in C57BL/6J

mice lies prior to K_{ATP} channel closure, at the level of beta cell glucose metabolism. These results are supported by genetic mapping data that rule out an involvement of the K_{ATP} channel subunit genes *Kir6.2* and *SUR1*, which map to mouse chromosome 7, outside the glucose tolerance loci identified here (data not shown).

Metabolism of glucose by the pancreatic beta cell is required for stimulation of insulin secretion by glucose (the main physiological determinant) (reviewed in Ref. [47]). Consequently, we studied *Gck*, a strong candidate gene located in the *Gluchos2* candidate region. This is a high K_M hexokinase that is rate-limiting for glycolysis and is strongly expressed in beta cells and liver. Its importance in insulin secretion is exemplified by the fact that homozygous mutations cause permanent neonatal diabetes in man [36] and heterozygous mutations cause an early-onset form of diabetes (MODY2) [32–37]. Previous work [6] has suggested that C57BL/6J mice secrete less insulin during an intravenous glucose tolerance test and have lower in vitro *Gck* protein activity (but similar protein levels) than DBA/2 mice. We therefore compared glucokinase in vitro phosphorylation activity in C57BL/6J and C3H/HeH mice. C57BL/6J mice had significantly lower glucokinase activity than C3H/HeH mice, despite similar (low) K_M hexokinase activity. We were unable to find any functional sequence changes to account for this, suggesting transcriptional or post-transcriptional regulation differences between the two mouse strains (however, it has been reported that *Gck* RNA levels are similar in these two strains [48]).

The *Gluchos1* candidate gene *Nnt* is a nuclear-encoded mitochondrial gene that functions as a redox-driven proton pump and catalyses the reversible reduction of $NADP^+$ by NADH [29]. Studies suggest that *Nnt* acts to buffer

NADPH levels by recruiting reducing equivalents from NAD-linked substrates during high demand for NADPH and limiting uncontrolled changes in metabolites associated with NAD-linked substrates [49]. Hoek and Rydstrom [49] propose that *Nnt* is important for integrating mitochondrial and cytosolic metabolism and for maintaining mitochondrial function under conditions of anoxia or high energy demand. It has also been argued that *Nnt* is involved in a substrate cycle with NAD- and NADP-linked isocitrate dehydrogenase, which contributes to regulation of the TCA cycle in mitochondria [50]. Recent studies have shown that an adequate supply of NAD(P)H to the mitochondria is necessary to generate the mitochondrial electrochemical gradient essential for ATP synthesis, and thereby insulin release [51]. In mice, *Nnt* is expressed to varying degrees in all cell types, and at the highest levels in kidney, testes, adrenal, liver, pancreas, bladder, lung, ovary and brain [52]. Given that glucose intolerance in susceptible humans develops with age, it is interesting that *Nnt* expression in mice declines more than twofold between 5 and 30 months, and is correlated with a typical decline in expression of other genes involved in mitochondrial bioenergetics [53].

Our studies revealed a mutation resulting in a missense (Met to Thr) mutation in the mitochondrial leader polypeptide of the *Nnt* precursor protein. We also found a five exon deletion in the C57BL/6J gene that removes four putative transmembrane helices and connecting linkers, and is expected to have a detrimental effect on protein function. Expression of *Nnt* RNA is more than sevenfold and fivefold lower in C57BL/6J liver and islets than in C3H/HeH control organs.

The nature of this mutation, its genomic position within the *Gluchos1* locus, the mitochondrial location, and the predicted biological role of *Nnt* [29, 49, 50, 54], coupled with the large difference in gene expression between the two strains, make it a strong candidate for the *Gluchos1* locus causal gene. The human NNT gene maps to 5p13.1-5cen; interestingly a genetic modifier of the age of diagnosis of MODY3 (an early-onset form of diabetes resulting from impaired insulin secretion) also maps to 5p15 [55].

At this stage we have no evidence for the nature of the gene underlying *Gluchos3* on chromosome 9.

In conclusion, impaired glucose tolerance in C57BL/6J mice is under the control of three main genes with several other genes having smaller effects. Our studies suggest that a large component of glucose insensitivity results from impaired glucose-stimulated insulin release due to defective beta cell metabolism. The deletion that we observed in the *Nnt* gene makes *Nnt* a strong causal candidate for *Gluchos1* and the reduced expression of *Gck* suggests it could be the gene underlying *Gluchos2*. We hypothesise that a mild reduction in glucokinase is compounded by a defect in mitochondrial metabolism that further reduces ATP production, leading to increased K_{ATP} currents and thus to the reduced insulin secretion that produces glucose intolerance. It seems possible that a similar deficiency in metabolism may contribute to the impaired insulin secretion found in human type 2 diabetes.

References

1. Straub SG, Sharp GW (2002) Glucose-stimulated signaling pathways in biphasic insulin secretion. Diabetes Metab Res Rev 18:451–463
2. Del Prato S (2003) Loss of early insulin secretion leads to postprandial hyperglycaemia. Diabetologia 46(Suppl 1):M2–M8
3. Bell GI, Polonsky KS (2001) Diabetes mellitus and genetically programmed defects in beta-cell function. Nature 414:788–791
4. Florez JC, Hirschhorn J, Altshuler D (2003) The inherited basis of diabetes mellitus: implications for the genetic analysis of complex traits. Annu Rev Genomics Hum Genet 4:257–291
5. Kaku K, Fiedorek FT Jr, Province M, Permutt MA (1988) Genetic analysis of glucose tolerance in inbred mouse strains. Evidence for polygenic control. Diabetes 37:707–713
6. Kooptiwut S, Zraika S, Thorburn AW et al (2002) Comparison of insulin secretory function in two mouse models with different susceptibility to beta-cell failure. Endocrinology 143:2085–2092
7. Surwit RS, Kuhn CM, Cochrane C, McCubbin JA, Feinglos MN (1988) Diet-induced type II diabetes in C57BL/6J mice. Diabetes 37:1163–1167
8. Surwit RS, Seldin MF, Kuhn CM, Cochrane C, Feinglos MN (1991) Control of expression of insulin resistance and hyperglycemia by different genetic factors in diabetic C57BL/6J mice. Diabetes 40:82–87
9. Burcelin R, Crivelli V, Dacosta A, Roy-Tirelli A, Thorens B (2002) Heterogeneous metabolic adaptation of C57BL/6J mice to high-fat diet. Am J Physiol Endocrinol Metabol 282:834–842
10. Fueger P, Bracy D, Malabanan C, Pencek R, Granner D, Wasserman D (2004) Hexokinase II overexpression improves exercise-stimulated but not insulin-stimulated muscle glucose uptake in high-fat-fed C57BL/6J mice. Diabetes 53:306–314
11. Surwit R, Feinglos M, Rodin J et al (1995) Differential effects of fat and sucrose on the development of obesity and diabetes in C57BL/6J and A/J Mice. Metabolism 44:645–651
12. Petro A, Cotter J, Cooper D, Peters J, Surwit S, Surwit R (2004) Fat, carbohydrate, and calories in the development of diabetes and obesity in the C57BL/6J Mouse. Metabolism 53:454–457
13. Black B, Croom J, Eisen E, Petro A, Edwards C, Surwit R (1998) Differential effects of fat and sucrose on body composition in A/J and C57BL/6 mice. Metabolism 47:1354–1359
14. Rossmeisl M, Rim JS, Koza RA, Kozak LP (2003) Variation in type 2 diabetes-related traits in mouse strains susceptible to diet-induced obesity. Diabetes 52:1958–1966
15. Goren H, Kulkarni R, Kahn C (2004) Glucose homeostasis and tissue transcript content of insulin signalling intermediates in four inbred strains of mice: C57BL/6, C57BLKS/6, DBA/2, and 129X1. Endocrinology 145:3307–3323
16. Kayo T, Fujita H, Nozaki J, Xiaofei E, Koizumi A (2000) Identification of two chromosomal loci determining glucose intolerance in a C57BL/6J mouse strain. Comp Med 50:296–302
17. Ahren B, Pacini G (2002) Insufficient islet compensation to insulin resistance vs. reduced glucose effectiveness in glucose-intolerant mice. Am J Physiol Endocrinol Metabol 283:E738–E744

18. Reimer M, Ahren B (2002) Altered beta-cell distribution of pdx-1 and GLUT-2 after a short-term challenge with a high fat diet in C57BL/6J Mice. Diabetes 51:S138–S143

19. Stoehr JP, Nadler ST, Schueler KL et al (2000) Genetic obesity unmasks nonlinear interactions between murine type 2 diabetes susceptibility loci. Diabetes 49:1946–1954

20. Fourmestraux V, Neubauer H, Poussin C et al (2004) Transcript profiling suggests that differential metabolic adaptation of mice to high fat diet is associated with changes in liver to muscle lipid fluxes. J Biol Chem 279:50743–50753

21. Dietrich WF, Miller JC, Steen RG et al (1994) A genetic map of the mouse with 4,006 simple sequence length polymorphisms. Nat Genet 7(Special issue):220–245

22. Manly KF, Cudmore RH Jr, Meer JM (2001) MapManager QTX, cross-platform software for genetic mapping. Mamm Genome 12:930–932

23. Lander E, Kruglyak L (1995) Genetic dissection of complex traits guidelines for interpreting and reporting linkage results. Nat Genet 11:241–247

24. Rorsman P, Trube G (1985) Glucose dependent K⁺-channels in pancreatic beta-cells are regulated by intracellular ATP. Pflügers Arch 405:305–309

25. Sakura H, Ashcroft SJH, Terauchi Y, Kadowaki T, Ashcroft FM (1998) Glucose modulation of ATP-sensitive K-currents in wild-type, homozygous and heterozygous glucokinase knock-out mice. Diabetologia 41:654–659

26. Gauguier D, Froguel P, Parent V et al (1996) Chromosomal mapping of genetic loci associated with non-insulin dependent diabetes in the GK rat. Nat Genet 12:38–43

27. Ashcroft, FM Kakei M (1989) ATP-sensitive K-channels: modulation by ATP and Mg^{2+} ions. J Physiol 416:349–367

28. Tucker SJ, Gribble FM, Zhao C, Trapp S, Ashcroft FM (1997) Truncation of Kir6.2 produces ATP-sensitive K-channels in the absence of the sulphonylurea receptor. Nature 387:179–183

29. Arkblad E, Betsholtz C, Rydstrom J (1996) The cDNA sequence of proton-pumping nicotinamide nucleotide transhydrogenase from man and mouse. Biochim Biophys Acta 1273:203–205

30. Arkblad EL, Betsholtz C, Mandoli D, Rydstrom J (2001) Characterization of a nicotinamide nucleotide transhydrogenase gene from the green alga Acetabularia acetabulum and comparison of its structure with those of the corresponding genes in mouse and Caenorhabditis elegans. Biochim Biophys Acta 1520:115–123

31. Kanemoto N, Hishigaki H, Miyakita A et al (1998) Genetic dissection of "OLETF", a rat model for non-insulin-dependent diabetes mellitus. Mamm Genome 9:419–425

32. Stoffel M, Froguel P, Taked J et al (1992) Human glucokinase gene: isolation, characterization, and identification of two missense mutations linked to early-onset non-insulin-dependent (type 2) diabetes mellitus. Proc Natl Acad Sci U S A 89:7698–7702

33. Velho G, Blanche H, Vaxillaire M et al (1997) Identification of 14 new glucokinase mutations and description of the clinical profile of 42 MODY-2 families. Diabetologia 40:217–224

34. Byrne M, Sturis J, Clement K et al (1994) Insulin secretory abnormalities in subjects with hyperglycemia due to glucokinase mutations. J Clin Invest 93:1120–1130

35. Hattersley AT, Turner RC, Permutt MA et al (1992) Linkage of type 2 diabetes to the glucokinase gene. Lancet 339:1307–1310

36. Njolstad PR, Sovik O, Cuesta-Munoz A et al (2001) Neonatal diabetes mellitus due to complete glucokinase deficiency. N Engl J Med 344:1588–1592

37. Vionnet N, Stoffel M, Takeda J et al (1992) Nonsense mutation in the glucokinase gene causes early-onset non-insulin-dependent diabetes mellitus. Nature 356:721–722

38. Leiter EH, Reifsnyder PC, Flurkey K, Partke HJ, Junger E, Herberg L (1998) NIDDM genes in mice: deleterious synergism by both parental genomes contributes to diabetogenic thresholds. Diabetes 47:1287–1295

39. Hirayama I, Yi Z, Izumi S et al (1999) Genetic analysis of obese diabetes in the TSOD mouse. Diabetes 48:1183–1191

40. Kim JH, Sen S, Avery CS et al (2001) Genetic analysis of a new mouse model for non-insulin-dependent diabetes. Genomics 74:273–286

41. Mehrabian M, Wong J, Wang X et al (2001) Genetic locus in mice that blocks development of atherosclerosis despite extreme hyperlipidemia. Circ Res 89:125–130

42. Suto J, Sekikawa K (2002) A quantitative trait locus that accounts for glucose intolerance maps to chromosome 8 in hereditary obese KK-A(y) mice. Int J Obes 26:1517–1519

43. Almind K, Kulkarni R, Lannon SM Kahn SR (2003) Identification of interactive loci linked to insulin and leptin in mice with genetic insulin resistance. Diabetes 52:1534–1535

44. Kido Y, Philippe N, Schaffer A, Accili D (2000) Genetic modifiers of the insulin resistance phenotype in mice. Diabetes 49:589–596

45. Bratanova-Tochkova TK, Cheng H, Daniel S et al (2002) Triggering and augmentation mechanisms, granule pools, and biphasic insulin secretion. Diabetes 51(Suppl 1):S83–S90

46. Kido Y, Burks D J, Withers D et al (2000) Tissue-specific insulin resistance in mice with mutations in the insulin receptor, IRS-1, and IRS-2. J Clin Invest 105:199–205

47. Persaud S, Howell S (2003) The biosynthesis and secretion of insulin. In: Pickup J, Williams G (eds) Textbook of diabetes. Blackwell, Oxford, pp 13.1–13.17

48. Moates J, Postic C, Decaux J, Girard J, Magnuson M (1997) Variable expression of hepatic glucokinase in mice is due to a regulational locus that co-segregates with the glucokinase gene. Genomics 45:185–193

49. Hoek JB, Rydstrom J (1988) Physiological roles of nicotinamide nucleotide transhydrogenase. Biochem J 254:1–10

50. Sazanov LA, Jackson JB (1994) Proton-translocating transhydrogenase and NAD- and NADP-linked isocitrate dehydrogenases operate in a substrate cycle which contributes to fine regulation of the tricarboxylic acid cycle activity in mitochondria. FEBS Lett 344:109–116

51. Tan C, Tuch BE, Tu J, Brown SA (2002) Role of NADH shuttles in glucose-induced insulin secretion from fetal β-cells. Diabetes 51:2989–2996

52. Arkblad EL, Egorov M, Shakhparonov M, Romanova L, Polzikov M, Rydstrom J (2002) Expression of proton-pumping nicotinamide nucleotide transhydrogenase in mouse, human brain and C elegans. Comp Biochem Physiol B Biochem Mol Biol 133:13–21

53. Lee CK, Klopp RG, Weindruch R, Prolla TA (1999) Gene expression profile of aging and its retardation by caloric restriction. Science 285:1390–1393

54. Wollheim CB, Maechler P (2002) Beta-cell mitochondria and insulin secretion-messenger role of nucleotides and metabolites. Diabetes 51(Suppl 1):S37–S42

55. Kim SH, Ma X, Klupa T et al (2003) Genetic modifiers of the age at diagnosis of diabetes (MODY3) in carriers of hepatocyte nuclear factor-1alpha mutations map to chromosomes 5p15, 9q22, and 14q24. Diabetes 52:2182–2186